Proceedings of the ASME 2023 18th International Manufacturing Science and Engineering Conference
MSEC2023
June 12-16, 2023, New Brunswick, New Jersey

MSEC2023-104372

EFFECT OF BLOWN POWDER DIRECTED ENERGY DEPOSITION ANGLE ON OVERSPRAY CONTAMINATION

Lauren Heinrich
Oak Ridge National Laboratory, Manufacturing Science Division, 2350 Cherahala Blvd, Knoxville, TN 37932, USA

Rangasayee Kannan
Oak Ridge National Laboratory, Manufacturing Science Division, 2350 Cherahala Blvd, Knoxville, TN 37932, USA

Alan Burl
Georgia Institute of Technology, Mechanical Engineering, Atlanta, GA 30332, USA

Peeyush Nandwana
Oak Ridge National Laboratory, Materials Science and Technology Division, 2350 Cherahala Blvd, Knoxville, TN 37932, USA

Kenton Fillingim
Oak Ridge National Laboratory, Manufacturing Science Division, 2350 Cherahala Blvd, Knoxville, TN 37932, USA

Thomas Feldhausen
Oak Ridge National Laboratory, Manufacturing Science Division, 2350 Cherahala Blvd, Knoxville, TN 37932, USA

Thomas Kurfess
Georgia Institute of Technology, Mechanical Engineering, Atlanta, GA 30332, USA

Christopher Saldaña
Georgia Institute of Technology, Mechanical Engineering, Atlanta, GA 30332, USA

ABSTRACT

Blown powder directed energy deposition (DED) hybrid machine tools are particularly beneficial when the net shape of a component is to be manufactured in an additive and machined interleaved fashion. This investigation seeks to analyze the effect of the additive head lean angle relative to the part on blown powder DED surface contamination due to overspray. These hybrid DED platforms are commonly installed on multi-axis machining systems where the lean of the deposition head relative to the component surface can be controlled by tilting the component. The blown powder DED process has a 10-50% lower catchment efficiency as compared to wire fed DED systems. This excess powder is still fed towards the deposition location where the particles are heated by the laser and rebound off the melt pool. Some of these heated particles impact the previously machined thin-wall surface. While the deposition process and tool path planning process has been evaluated, the effect of the overspray due to lean angle of the deposition head on the previously thin-wall machined surface is not yet fully understood. This investigation found that minimum lean angle coincides with minimal overspray effect with nearly no contamination. If a lean angle is required, the maximum lean angle possible should be implemented for the smallest effected overspray area on the machined surface which was found to decrease the affect zone by half compared to intermediate lean angles. A diameter divergence was also noticed as the deposition angle was increased. In this study, a thorough analysis of the surface and geometric effects when depositing thin-walled components at varying angles is completed. It has been shown that part quality can be significantly affected by lean angle and thus must be incorporated as an additional design consideration in the manufacturing process.

Keywords: Directed Energy Deposition, Hybrid Manufacturing, Blown Powder Directed Energy Deposition

NOMENCLATURE

AM	Additive Manufacturing
DED	Directed Energy Deposition

1. INTRODUCTION

Hybrid manufacturing is beneficial due to the capability of interleaving additive and subtractive tool cycles within the same machine tool without re-fixturing [1-4]. The interleaving of processes enabled by hybrid manufacturing provides an efficient solution for high aspect ratio components by decreasing the need for complex 5-axis tool paths and long reach tooling [5, 6]. Many of these hybrid machines integrate directed energy deposition (DED) systems for the metal additive processing system [7-10]. The AM process enables the near net shape manufacture of components with increased material efficiency and geometric flexibility for high buy-to-fly components [11-13]. These DED processes often do not have the required surface resolution for final component service, whereas the subtractive processing system native to the machine tool enables the manufacture of components with high-quality surface finish [14].

DED AM systems on hybrid machine tools use either powder or wire metals as feedstock, alongside electric arc or laser heat sources [15-17]. Blown powder DED systems use a carrier gas to deliver metal powder from the feeding system to the deposition location, where it is melted by a laser [18]. The ratio of injected powder to material captured in the melt pool is defined as the powder catchment efficiency and ranges from 50-80% for a typical powder DED process [19]. Some researchers have evaluated ways to increase the catchment efficiency while other have assessed the feasibility of powder re-use [19, 20].

A portion of incident powder on the melt pool rebounds away, thus resulting in powder overspray [21]. The most efficient powder catchment occurs when the convergence point of the powder is stable at the melt pool location [22]. This is possible when the actual layer height is programmed equal to the deposited layer height. However, the deposited layer height is dependent on several factors, such as material flow, residual heat, traverse speed, and added heat [23]. Even with ideal deposition parameters, some of the powder that is not caught in the melt pool is heated by the laser, then impacts the surrounding structure. These particles can stick to surrounding surfaces depending on the particle temperature, distance traveled, and deposition head lean. This processing affect should be taken into account when interleaving with hybrid manufacturing.

The hybrid interleaving process is ideally designed such that the machined section does not have to be re-machined after consecutive deposition sections for reduced cycle time. However, with blown powder hybrid 5-axis systems, the tool path planner can determine the lead and lean of the deposition head relative to the component for a decreased need for support material [24]. While lead and lean are typically defined as the tool orientation relative to the component, in this investigation, the part will be tilted, or set at a lean angle, in relation to the deposition head that is always kept vertical, or in-line with gravity. This angle adjustment alters the excess particles' trajectory versus the component surface. Researchers have evaluated the change in yield strength at varied deposition angles and recognized that overspray can be an issue with component quality, however, no studies have quantified the effect of overspray on hybrid component surface quality [3, 25, 26].

In this study, the influence of the deposition head lean relative to the component overspray contamination on the previously machined surface is investigated. The experimental setup to evaluate the effect of overspray is described, the process parameter development is discussed, and the results of the component analysis is reported in this study. It was found that a minimum lean angle created the least overspray contamination on the previously machined vertical section. Additionally, a maximum angle isolated contamination to the upper-most section of the machined component, decreasing the affected area by half as compared to the other lean angles. A correlation between an increase in lean angle and increase in diameter divergence was also found during the experimental process.

2. MATERIALS AND METHODS

A hybrid manufacturing system that uses blown powder DED is used to fabricate near-net shape components that can be machined in sections during the build-up process. For this investigation, a Mazak VC-500 AM blown powder hybrid machine tool with an IPG Photonics YLS-1000-CUT fiber laser as the heat source focused with a 1.2 mm spot size and coaxially fed powder was used. A representation of the deposition head can be seen in Figure 1. Argon was used as the shielding, powder stream carrier, and inner laser nozzle cover gas whereas Oerlikon MetcoAdd 316L-D -106+45 µm powder was used as the feedstock.

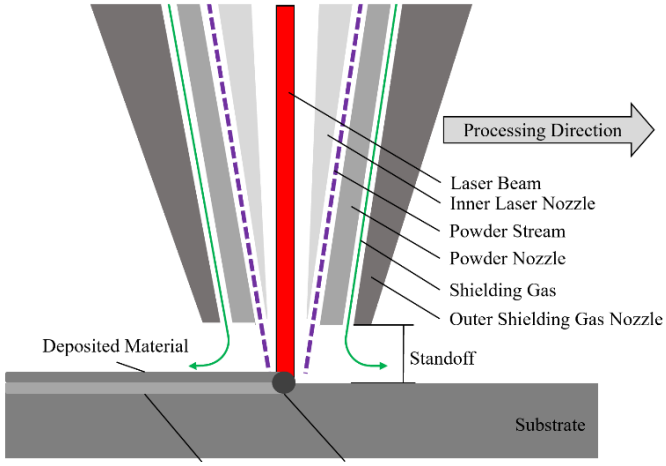

FIGURE 1: COAXIAL BLOWN POWDER DED NOZZLE COMPONENT DIAGRAM.

A single bead tube having a center-line diameter of 30 mm was deposited and machined to a uniform thickness of 1 mm and height of 15 mm. A second single bead tube having dimensions identical to those of the initial build was deposited on the initial tube with varying lean angles. The dimensions of each segment can be seen in Figure 2A. These steps can be seen in Figure A1, and the machine kinematic layout can be seen in Figure A2 in the Appendix. The deposition parameters are shown in Table 1. A helical tool path was used, so there was a continuous single bead for each 15 mm section of the component, as shown in Figure A3 of the Appendix. A 304 stainless steel hot-rolled 76mm square plate machined flat 6 mm thick was the substrate due to its weldability between 316 stainless steel. The sample geometry dimensions can be seen in Figure 2A. For each lean angle, a total of four specimens were manufactured. Two of the specimens were solid, with the other two having a 25 mm hole concentric with the tube. The hole was included to analyze the affect powder escape would have on the internal surface roughness.

TABLE 1: DEPOSITION PARAMETERS

Parameter	Value	Unit
Layer height	0.59	mm
Traverse speed	250	mm/min
Powder feed	3.1	g/min
Section 1 laser power	352	Watts
Section 2 laser power	295	Watts
Lean angles	0.1, 13.3, 26.6, 40	Degrees

The deposition process utilized a 3+2 axis configuration where the B-axis of the table was tilted outward relative to the part at the desired deposition angle, as can be seen in in Figure 2B. The C-axis was set to rotate at a given speed, and the X, Y, and Z linear axes simultaneously moved for a smooth, helical deposition tool path. While the component was still fixtured in the machine, the inside of the machined section of the tube was probed with a Renishaw RMP-600 probe, with the bore probing macro cycle at 4, 8.5, and 13 mm from the top of the substrate before and after the angled top section was deposited. The probe has a repeatability of 0.25 μm at 2σ [27]. The deposited tubes can be seen in Figure A4 of the Appendix.

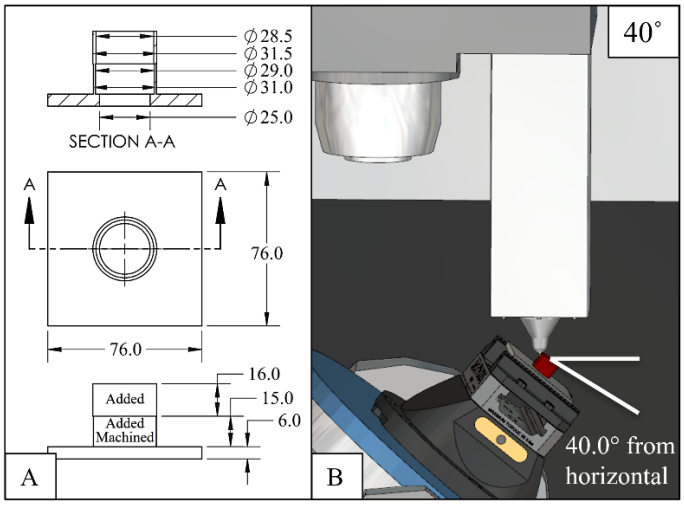

FIGURE 2: A) DIMENSIONED DEPOSITED GEOMETRY WITH THE SUBSTRATE WITH A HOLE SHOWN IN MM AND B) THE MACHINE KINEMATIC CONFIGURATION AT THE 40.0-DEGREE LEAN ANGLE

After manufacturing, the surface roughness of the machined section was evaluated using a Mitutoyo SJ-411 surface profilometer. The profilometry settings can be seen in Table 2. The inside and outside surfaces were evaluated at four increments around the tube, approximately 90-degrees apart and the results were averaged between each two identical samples.

TABLE 2: PROFILOMETRY PARAMETERS

Parameter	Value	Unit
Standard	ANSI	-
Profile	R	-
Parameter	6	-
Filter	Gaussian	-
λc	0.8	mm
λs	2.5	μm
Number of segments	15	-

During the analysis, it was apparent that the upper section of the deposited tube was a larger diameter than the machined section, as seen in Figure 5A versus Figure 5D. The outer-most diameter was measured for each sample. Additionally, the 0.1 degree and 40.0-degree tubes were scanned with a Zeiss Comet L3D light scanner. The 3-dimensional divergence from the ideal finished geometry was performed using Volume Graphics.

This evaluation seeks to correlate the lean angle to the amount of overspray contamination on the previously machined section. It also seeks to determine the effect of deposition angle on the increase in diameter of the upper deposited section. Samples were geometrically evaluated with both on-machine probing and light scanning. The surface properties were evaluated with surface profilometry, and the geometric divergence was evaluated with manual measurement and light scanning.

3. RESULTS AND DISCUSSION

Four angles were evaluated between 0.1 to 40.0 degrees of B-axis tilt while the deposition head stays vertical in the Z axis direction as can be seen in Figure 2B. Two components were manufactured with the same deposition parameters and substrate conditions at each angle. The two substrate conditions were a solid substrate and a substrate with a 25 mm hole drilled in the middle to allow the particles to escape through the bottom of the substrate as can be seen in Figure 2A. The first quantitative evaluation was the evaluation of the change in the inner tube diameter before and after the upper tube section was deposited with on-machine probing. It was found the uppermost section of the machined tube did contract due to the residual stress induced by the solidification process. To determine the amount of over spray contamination at the four different angles, the surface roughness of the machined section was evaluated using surface profilometry. It was found that a minimum or maximum angle should be used to nearly prevent or isolate the contamination near the new additive section, respectively. At the minimum angle where the deposition head is colinear with the deposition direction, the powder flow is slightly diverged by the previous section preventing any collision of the powder particles with the previously machined section. At the maximum angle, the collision trajectory is isolated to the upper-most section of the previously machined section enabling less machining to remove the contamination. It was also found the tube deposited at the largest angle diverged the most. The authors believe this divergence could be due to stacking of the deposited beads

during a slightly over-building condition where the programmed layer height is slightly less than the actual deposited layer height causing a diverging geometry effect.

3.1 Probing Results

Step two of the component manufacturing was machining the first section of deposited tube to 1 mm wall thickness with an outside diameter of 31 mm and an inside diameter of 29 mm. After the machining, the inside of the tube was probed with the Renishaw bore probing macro cycle at 4, 8.5, and 13 mm from the substrate. After the upper section of the tube was deposited, the inside was probed again at the same locations and the results of the probing difference can be seen in Figure 3. The labeling of the data in Figure 3 is described here; two components of each condition were manufactured where the first number represents the angle of deposition, the second number represents whether it was the first or second of each component, and the S or H represent if the substrate was solid or had a 25 mm hole drilled in the center. For example, the first value represented by 0.1x1S was a sample deposited at an angle of 0.1 degrees, was the first sample with a solid substrate.

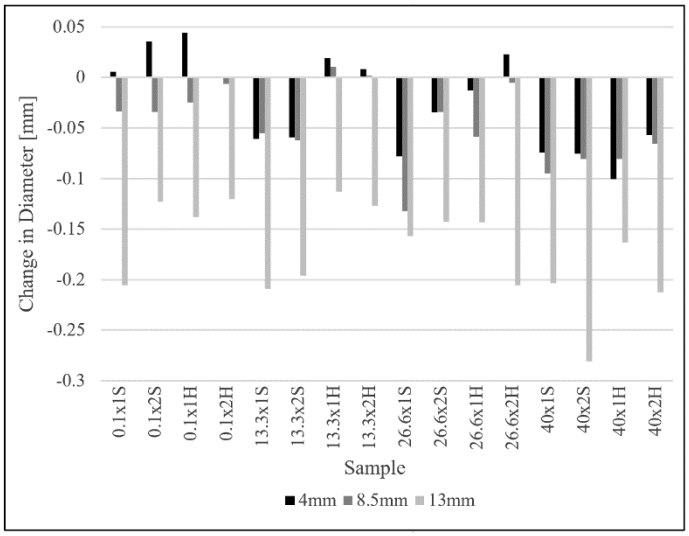

FIGURE 3: TUBE DIAMETER PROBING RESULTS AT 4, 8.5, AND 13 MM FROM THE SUBSTRATE SHOWING THE DECREASE IN DIAMTER AFTER DEPOSITION

The tubes manufactured on substrates with holes, on average, deflected less, than the solid substrate tubes as can be seen in Figure 3. The angle of the deposition had a lesser effect on the magnitude of deflection. The tubes had minimal deflection near the bottom of the tube due to the rigidity of the substrate as compared to the top of the machined sections furthest from extra support. The most deflection occurred closest to the deposition interface between steps two and three with the thin wall thickness. As the deposited material cooled and contracted, the lower section deflected indicating a need for a better understanding of interface deflection and how to compensate for interface misalignment for the manufacture of geometrically accurate interleaved hybrid manufactured components.

3.2 Surface Roughness Results

Next, the surface roughness of the previously machined surface was evaluated. The surface roughness was quantitatively evaluated with surface profilometry and an example of the profile between each deposition angle can be seen in Figure 4. It was qualitatively observed that the surface contamination was related to the lean angle of the deposition head as can be seen in Figure 5 as well as in Figure A4 of the Appendix. Haley et al. showed the powder particles of the blown powder system can be treated like the carrier gas for trajectory prediction purposes [20]. With this assumption in mind, the particle trajectory is accepted to be the same as the coaxial gas flow where the gas converges then continues in a straight line colinear with the laser beam. The gas flow is then deflected by the substrate or the previously machined geometry. As the lean angle is increased, the fluid divergence increases as well. The surface profilometry results show minimal overspray effect at the least angle whereas increased angles cause an increase in overspray contamination. As the angle increased, the length of the contaminated machined surface decreased, but the local concentration of the particles increased as can be seen in Figure 4 which is a single surface profile plot chosen from one sample at each lean angle. A more comprehensive comparison can be seen in Figure A5 of the Appendix.

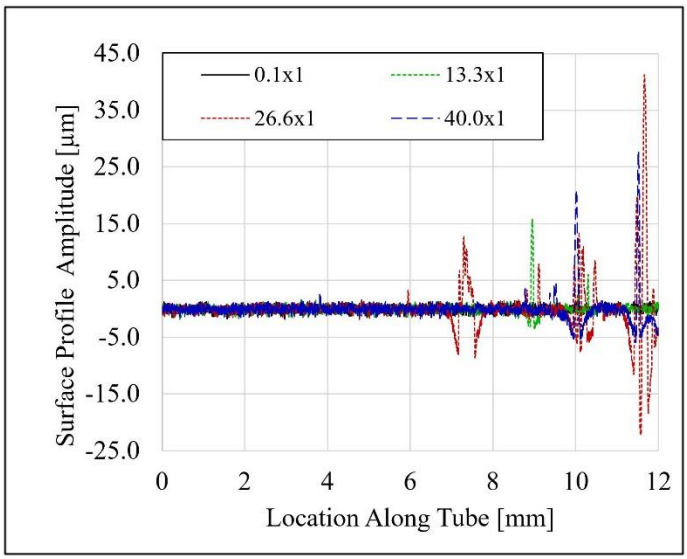

FIGURE 4: SURFACE PROFILOMETER SIDE 1 OUTSIDE PROFILE RESULTS COMPARING THE CONTAMINATION DIASTANCE ALONG THE TUBE SURFACE

The dip in the profile before each high-amplitude point indicates the particle partially melted and imbedded itself into the machine surface. The graph of the surface profilometry results from side one of each sample shows how the particles were distributed along the top of the tube as the angle increased in Figure 4. Then, at the maximum angle, the surface roughness was isolated to the top of the machined section. This is due to the increased lean of the part relative to the deposition head causing the fluid flow to rebound off the machined surface more directly

rather than flow along the machined surface for the components manufactured at 13.3 and 26.6-degrees. An optical qualitative example of the change in surface quality can be seen in Figure 5 A versus B where A was deposited at 0.1-degrees and B was deposited at 26.6-degree lean.

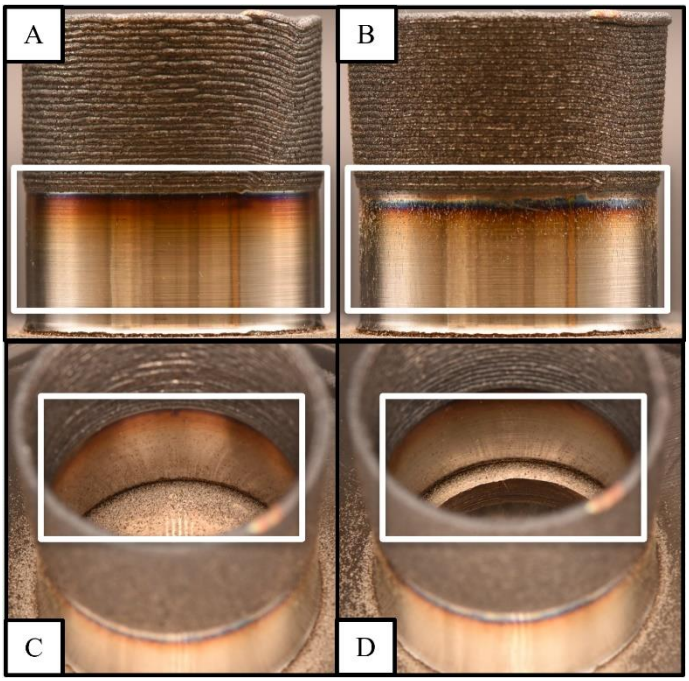

FIGURE 5: QUALITATIVE OVERSPRAY CONTAMINATION COMPARISON OF THE OUTSIDE COMPARING A) 0.1-DEGREE LEAN VERSUS B) 26.6-DEGREE LEAN AS WELL AS THE REBOUND EFFECT CAUSED BY A C) SOLID SUBSTRATE VERSUS A D) SUBSTRATE WITH A THROUGH-HOLE AT 26.6-DEGREE LEAN

The results of the inside roughness show that the through-hole allowed some of the particles to escape when the deposition angle was small as can be seen in Figure 5C and 5D; however, at the higher angles, the surface roughness was nearly identical to that of the solid substrate as can be seen in Figure 6.

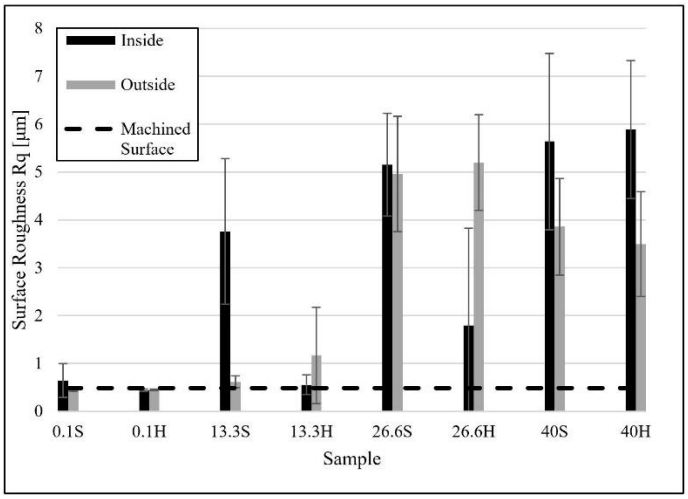

FIGURE 6: SURFACE PROFILOMETER ROUGHNESS RESULTS FOR THE INSIDE VERSUS OUTSIDE TUBE SURFACE AT EACH ANGLE

The 0.1-degree deposition had nearly no contamination as indicated quantitatively in Figure 6 as well and qualitatively in Figure 5A. The low levels of contamination are due to the top, flat machined surface of section 1 diverges the fluid flow enough that the particles do not impact the lower surface of the machined section. The inner contamination is also limited due to the direct rebound of the particle from the substrate and not into the tube walls. The 13.3-degree deposition had an increased level of contamination on the tube. As can be seen in Figure 4, that contamination extended to about 1/3 of the way down the machined surface, however, it was not as far as the 26.6-degree deposition that had a much more direct fluid flow into the side of the machined surface as can be seen in Figure 5B. The inside of the solid substrate had a steep increase in roughness as compared to the 0.1-degree deposition as the fluid and particles are angled towards the substrate surface at an angle and have nowhere to escape whereas the 13.3-degree substrate with a hole has negligible roughness. At 26.6-degrees of lean, the outer surface had the most contamination along the surface as can be seen in the qualitative results of Figure 5, as well as quantitatively in the surface profile of Figure 4 and the surface roughness value in Figure 6. The substrate with a hole did offer some escape of the particles through the bottom, decreasing the inner contamination as compared to the solid substrate. Finally, the 40.0-degree deposition has the most contamination, however, it was isolated near the deposited section. The increased angle will prevent the substrate from becoming contaminated with overspray and minimal machining is required from the interleaved added section to meet required surface finish expectations. There was also a negligible difference between the solid substrate and the substrate with a hole indicating the angle was great enough that the hole was not effective at decreasing the overspray contamination of the inner tube at an angle of 40.0-degrees or greater.

3.3 Angled Deposition Divergence Results

Lastly, it was noticed the tube diameter diverged as the deposition lean angle increased. The laser scan comparison of the 0.01-degree deposition compared to the 40.0-degree deposition indicates there was a change in geometric accuracy as can be seen in Figure 7.

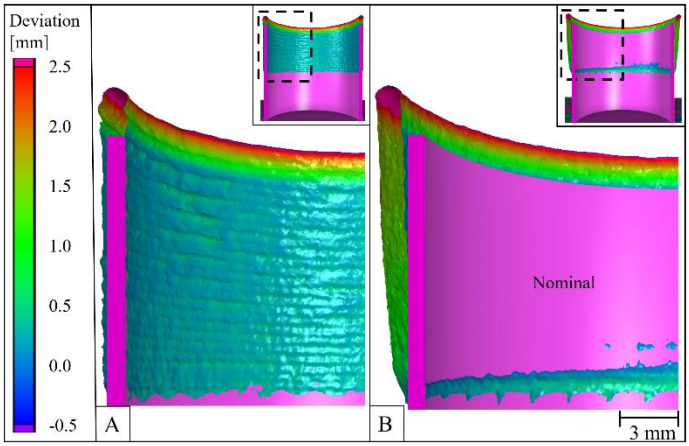

FIGURE 7: VOLUME GRAPHICS COMPARISON OF THE A) 0.1-DEGREE DEPOSITION VERSUS THE B) 40.0-DEGREE DEPOSITION WITH THE IDEAL MACHINED FINAL MAGENTA GEOMETRY

The divergence can be qualitatively observed in Figure A4 A-D in the appendix illustrating the divergence increased as the angle of deposition lean increased. Figure 8 quantitatively shows the increase in diameter as the deposition lean angle increases.

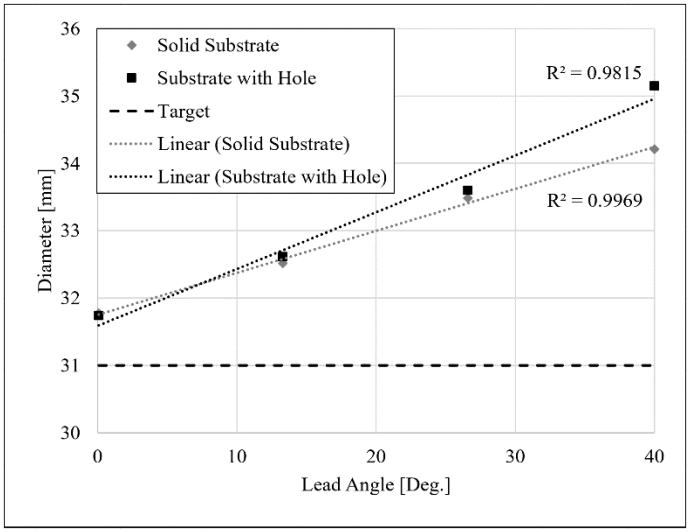

FIGURE 8: DEPOSITED TUBE DIAMETER DIVERGENCE

The phenomenon causing this divergence is unknown, but it will be investigated further through a 3-axis deposition where the C-axis is still and the X, Y, and Z axes are moved simultaneously to determine if the divergence was affected by gravity or some other solidification phenomenon.

4. CONCLUSION

The present study showed that blown powder DED lean angle affected overspray contamination. A minimal lean angle had the least contamination, and the maximum deposition lean angle isolates the contamination closest to the added section. The increase in diameter throughout the deposition process with the increased lean angle will be investigated further in future work.

ACKNOWLEDGEMENTS

The authors would like to acknowledge the cooperation and support of Mazak Corporation. The authors would also like to acknowledge Joseph Fletcher, Dennis Brown, Sarah Graham, and Andrés Márquez Rossy. Funding: This work is funded by the Department of Energy DE-EE0008303 with the support of Oak Ridge National Laboratory. This manuscript has been authored by UT-Battelle, LLC under Contract No. DE-AC05-00OR22725 with the U.S. Department of Energy. Research was co-sponsored by the U.S. Department of Energy, Office of Energy Efficiency and Renewable Energy, Advanced Manufacturing Office.

REFERENCES

[1] Cortina, M., Arrizubieta, J. I., Ruiz, J. E., Ukar, E., and Lamikiz, A., 2018, "Latest Developments in Industrial Hybrid Machine Tools that Combine Additive and Subtractive Operations," Materials (Basel), 11(12).

[2] Flynn, J. M., Shokrani, A., Newman, S. T., and Dhokia, V., 2016, "Hybrid additive and subtractive machine tools – Research and industrial developments," International Journal of Machine Tools and Manufacture, 101, pp. 79-101.

[3] Lorenz, K. A., 2015, "A Review of Hybrid Manufacturing," 2014 International Solid Freeform Fabrication Symposium The University of Texas at Austin.

[4] Yamazaki, T., 2016, "Development of A Hybrid Multi-tasking Machine Tool: Integration of Additive Manufacturing Technology with CNC Machining," Procedia CIRP, 42, pp. 81-86.

[5] Feldhausen, T., Raghavan, N., Saleeby, K., Love, L., and Kurfess, T., 2021, "Mechanical properties and microstructure of 316L stainless steel produced by hybrid manufacturing," Journal of Materials Processing Technology, 290.

[6] Soshi, M., Ring, J., Young, C., Oda, Y., and Mori, M., 2017, "Innovative grid molding and cooling using an additive and subtractive hybrid CNC machine tool," CIRP Annals, 66(1), pp. 401-404.

[7] Feldhausen, T., Saleeby, K., and Kurfess, T., 2021, "Spinning the digital thread with hybrid manufacturing," Manufacturing Letters, 29, pp. 15-18.

[8] Marin, F., de Souza, A. F., Ahrens, C. H., and de Lacalle, L. N. L., 2021, "A new hybrid process combining machining and selective laser melting to manufacture an advanced concept of conformal cooling channels for plastic injection molds," The International Journal of Advanced Manufacturing Technology, 113(5-6), pp. 1561-1576.

[9] Ren, L., 2006, "Three Dimensional Die Repair using a Hybrid Manufacturing System," 17th Annual Solid Freeform Fabrication Symposium, University of Texas at Austin, Austin, Texas.
[10] Saleeby, K., Feldhausen, T., Love, L., and Kurfess, T., 2020, "Rapid Retooling for Emergency Response with Hybrid Manufacturing," Smart and Sustainable Manufacturing Systems, 4(3).
[11] Rodrigues, T. A., Duarte, V., Miranda, R. M., Santos, T. G., and Oliveira, J. P., 2019, "Current Status and Perspectives on Wire and Arc Additive Manufacturing (WAAM)," Materials (Basel), 12(7).
[12] Ding, D., Pan, Z., Cuiuri, D., Li, H., and Larkin, N., 2016, "Adaptive path planning for wire-feed additive manufacturing using medial axis transformation," Journal of Cleaner Production, 133, pp. 942-952.
[13] Szost, B. A., Terzi, S., Martina, F., Boisselier, D., Prytuliak, A., Pirling, T., Hofmann, M., and Jarvis, D. J., 2016, "A comparative study of additive manufacturing techniques: Residual stress and microstructural analysis of CLAD and WAAM printed Ti–6Al–4V components," Materials & Design, 89, pp. 559-567.
[14] Feldhausen, T., 2020, "Development and Evaluation of Interfacial Structures for Hybrid Manufacturing," Doctor of Philosophy Dissertation, Georgia Institute of Technology.
[15] Mazzucato, F., Marchetti, A., and Valente, A., 2018, "Analysis of the Influence of Shielding and Carrier Gases on the DED Powder Deposition Efficiency for a New Deposition Nozzle Design Solution," Industrializing Additive Manufacturing - Proceedings of Additive Manufacturing in Products and Applications - AMPA2017, pp. 59-69.
[16] Wu, X., and Li, S., 2017, "Experimental investigations of a hybrid machining combining wire electrical discharge machining (WEDM) and fixed abrasive wire saw," The International Journal of Advanced Manufacturing Technology, 95(5-8), pp. 2613-2623.
[17] Dinovitzer, M., Chen, X., Laliberte, J., Huang, X., and Frei, H., 2019, "Effect of wire and arc additive manufacturing (WAAM) process parameters on bead geometry and microstructure," Additive Manufacturing, 26, pp. 138-146.
[18] Siva Prasad, H., Brueckner, F., and Kaplan, A. F. H., 2020, "Powder incorporation and spatter formation in high deposition rate blown powder directed energy deposition," Additive Manufacturing, 35.
[19] Takemura, S., Koike, R., Kakinuma, Y., Sato, Y., and Oda, Y., 2019, "Design of powder nozzle for high resource efficiency in directed energy deposition based on computational fluid dynamics simulation," The International Journal of Advanced Manufacturing Technology, 105(10), pp. 4107-4121.
[20] Terrassa, K. L., Haley, J. C., MacDonald, B. E., and Schoenung, J. M., 2018, "Reuse of powder feedstock for directed energy deposition," Powder Technology, 338, pp. 819-829.
[21] Haley, J. C., Schoenung, J. M., and Lavernia, E. J., 2018, "Observations of particle-melt pool impact events in directed energy deposition," Additive Manufacturing, 22, pp. 368-374.
[22] Haley, J. C., Zheng, B., Bertoli, U. S., Dupuy, A. D., Schoenung, J. M., and Lavernia, E. J., 2019, "Working distance passive stability in laser directed energy deposition additive manufacturing," Materials & Design, 161, pp. 86-94.
[23] Amine, T., Newkirk, J. W., and Liou, F., 2014, "An investigation of the effect of laser deposition parameters on characteristics of multilayered 316 L deposits," The International Journal of Advanced Manufacturing Technology, 73(9-12), pp. 1739-1749.
[24] Feldhausen, T., Heinrich, L., Saleeby, K., Burl, A., Post, B., MacDonald, E., Saldana, C., and Love, L., 2022, "Review of Computer-Aided Manufacturing (CAM) strategies for hybrid directed energy deposition," Additive Manufacturing, 56.
[25] Kersten, S. L., 2020, "Effect of Build Orientation of Anisotropic Behavior in Direct Energy Deposition Built Components," Master of Science, Georgia Institute of Technology.
[26] Gradl, P. R., Protz, C., Fikes, J., Ellis, D., Evans, L., Clark, A., Miller, S., and Hudson, T., 2020, "Lightweight Thrust Chamber Assemblies using Multi-Alloy Additive Manufacturing and Composite Overwrap," AIAA Propulsion and Energy 2020 Forum.
[27] 2022, "Machine tool probes and software," https://www.renishaw.com/en/rmp600-high-accuracy-machine-probe--8880.

APPENDIX

FIGURE A1: ADDITIVE PROCESSING OF THE HYBRID TUBE WHERE STEP ONE IS THE DEPOSITION OF THE FIRST SECTION OF TUBE WITH A CONTINUOUS TOOL PATH, STEP TWO IS THE MACHINING OF THE TUBE TO 1 MM WALL THICKNESS AND 31 MM OUTER DIAMETER, AND STEP THREE IS THE ADDITIVE DEPOSITION OF THE TUBE WITH THE SAME TOOL PATH AS STEP 1, BUT AT THE 4 LEAN ANGLES OF 0.1, 13.3, 26.6, AND 40.0 DEGREES. THE SAMPLE SHOWN WAS DEPOSITED AT 0.01 DEGREES LEAN

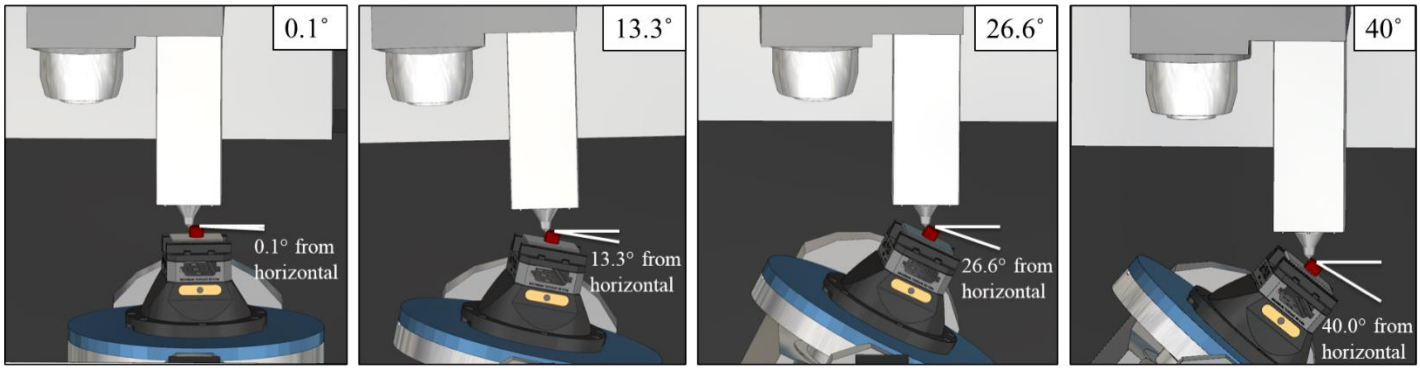

FIGURE A2: MACHINE KINEMATIC LAYOUT EACH OF THE FOUR DEPOSITION LEAN ANGLES UTILIZED DURING COMPONENT MANUFACTURE.

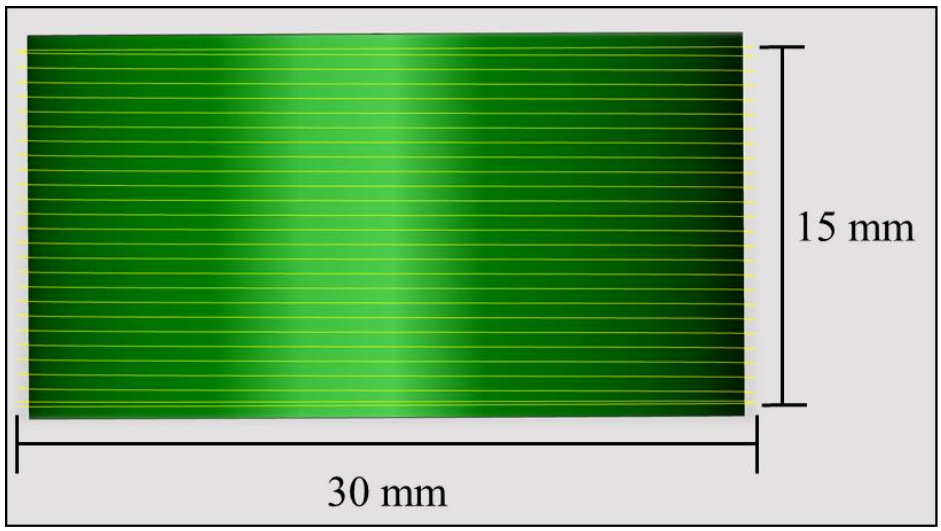

FIGURE A3: HELICAL DEPOSITION TOOL PATH

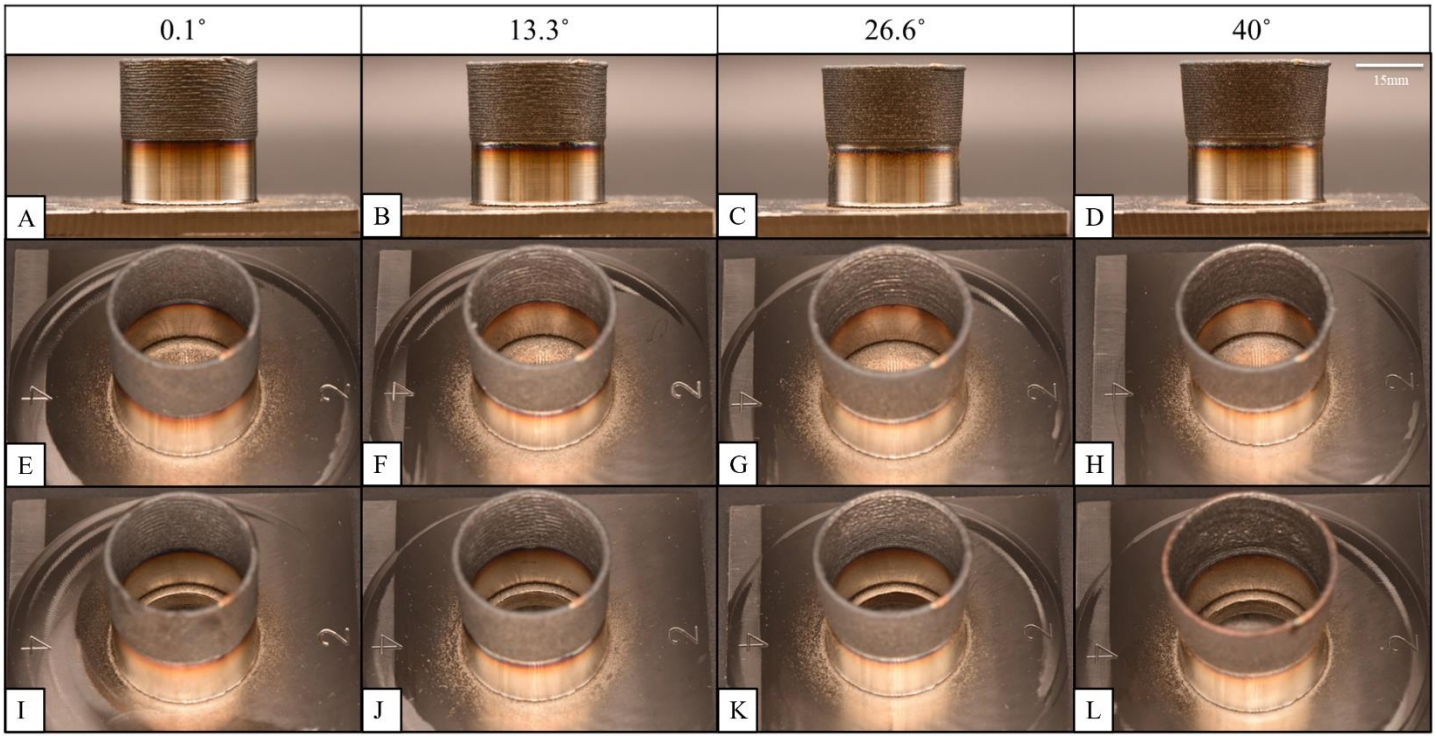

FIGURE A4: QUALITATIVE TUBE DEPOSITION RESULTS WHERE A-D) HORIZONTAL QUALITATIVE ANALYSIS AT EACH LEAN ANGLE, E-H) OBLIQUE QUALITATIVE ANALYSIS OF THE INSIDE OF THE MACHINED TUBE WITH A SOLID SUBSTRATE, AND I-L) OBLIQUE QUALISTATIVE ANALYSIS OF THE INSIDE OF THE MACHINED TUBE WITH A SUBSTRATE WITH A CONCENTRIC HOLE.

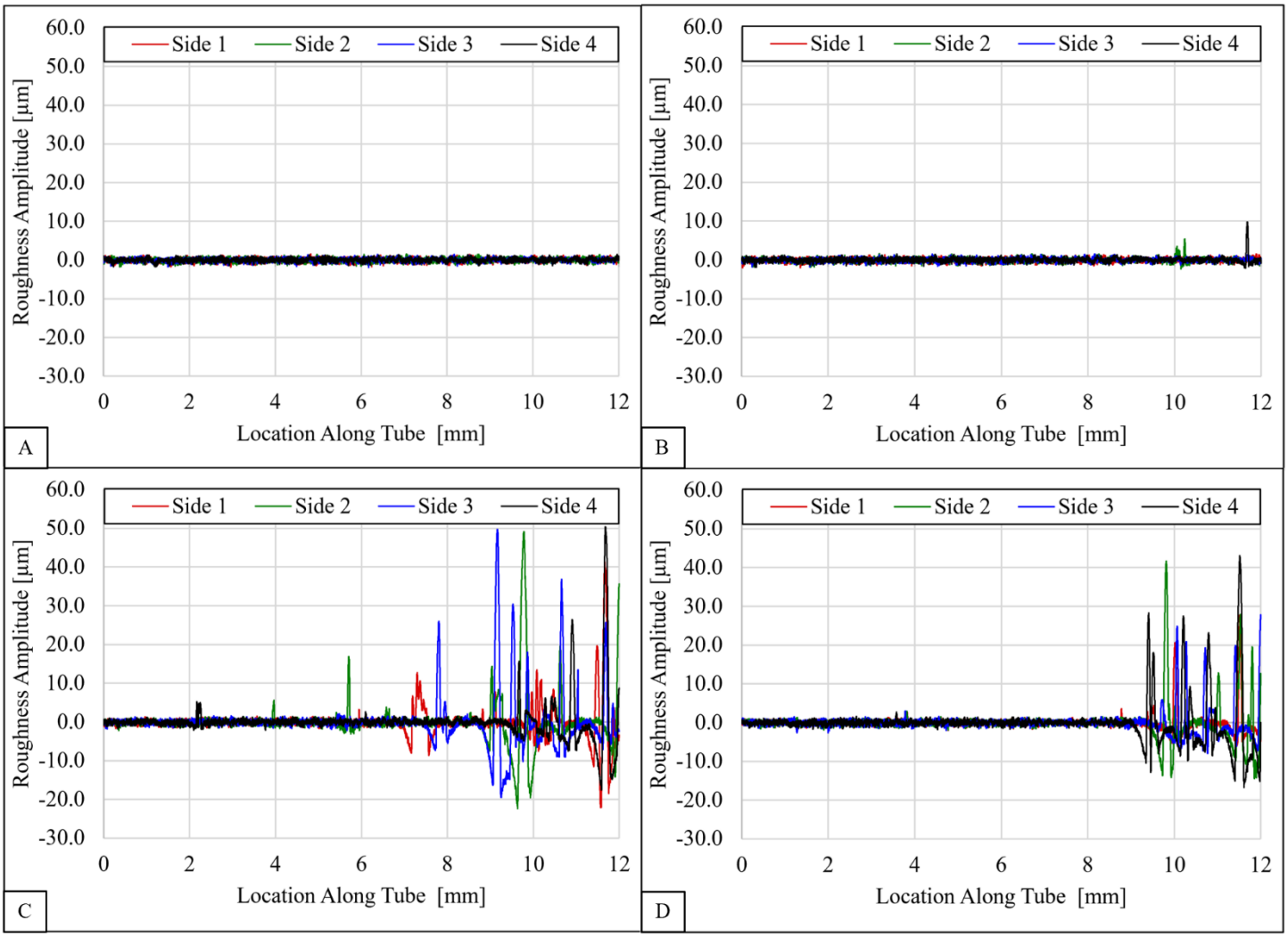

FIGURE A5: PROFILOMETER PROFILE GRAPHS OF FOUR MEASUREMENTS AROUND EACH TUBE AT 90 DEGREE SEPARATIONS AT A LEAN OF A) 0.1, B) 13.3, C) 26.6, AND D) 40 DEGREES.